

Global distribution of contrail radiative forcing

Patrick Minnis,¹ Ulrich Schumann,² David R. Doelling,³
Klaus M. Gierens,² and David W. Fahey⁴

Abstract. The global distribution of radiative forcing by persistent linear contrails has been estimated for 1992 and 2050 using global contrail cover computed for aircraft fuel consumption scenarios for the two periods, a detailed prescription of the radiative properties of the Earth's surface and the cloudy atmosphere, and flux computations with an established radiative transfer model. The computed global mean radiative forcing by line-shaped contrails is $\sim 0.02 \text{ Wm}^{-2}$ in 1992 and $\sim 0.1 \text{ Wm}^{-2}$ in 2050. At northern mid-latitudes, the zonal mean forcing is five times larger than the global mean. Diffuse contrails and indirect effects of aircraft emissions on natural cirrus are not included in this study. Thus, the results are considered a minimum estimate of contrail effects.

Introduction

Contrails are ice clouds with radiative effects similar to thin cirrus clouds [Schumann and Wendling 1990; Fu and Liou 1993]. They are short-lived when formed in dry air but persist and develop into extended cirrus cloud layers when the ambient relative humidity exceeds ice saturation. Individual contrails may persist for hours and develop into cirrus clouds indistinguishable from those formed naturally [Minnis *et al.* 1998]. Some climate model studies indicate that contrails may have significant regional radiative climatic impacts [e.g., Liou *et al.* 1990; Ponater *et al.* 1996]. While idealized cases have been examined [Fortuin *et al.* 1995; Meerkötter *et al.* 1999], more realistic studies of global and regional radiative forcing by contrails are needed to improve our understanding of the climatic effects of present and potential future air traffic.

Contrails that have a line-shaped structure can be readily identified in satellite data. On average, such line-shaped contrails annually cover 0.5 - 2% of parts of Europe and the Eastern North Atlantic [Bakan *et al.* 1994; Mannstein *et al.* 1998], but their global coverage has not yet been measured. Using meteorological and traffic data with the regional observations, the global mean cover by line-shaped contrails is estimated to be about 0.1% [Sausen *et al.* 1998]. These analyses together with satellite observations of persistent contrail patches [Mannstein *et al.* 1999], and in-situ measurements of ice saturation along upper-tropospheric airline routes [Gierens *et al.* 1999b], reveal that airliners cruise 10 to 20 % of the time in air masses that are cool and

humid enough for the formation of persistent contrails. The mean annual contrail frequency observed in the USA and aircraft fuel usage above 7-km altitude are well correlated [Minnis *et al.* 1997] indicating that contrail frequency will grow with air traffic, including areas with large traffic density. Global air traffic, in terms of passenger-kilometers flown, rose annually by 7.1% from 1994 to 1997. Air travel is expected to continue growing. Hence contrails will play a larger role in future climates than they do today.

In this paper, we use the currently available estimates of present and future contrail coverage and contrail radiative properties to provide the first estimate of the global distribution of contrail-induced radiative forcing.

Methods, Scenarios, and Contrail Cover

Radiative forcing by contrails over a given region is determined by computing the fluxes at the top of the atmosphere with and without contrails. The computations are performed separately for clear and cloudy conditions for each region. Contrail optical properties are held constant while the fractional coverage is specified for a given region. The contrail fractional coverage c is assumed to overlap randomly with other clouds. Thus, for a region with a fractional cloud cover C , the contrail forcing F for a given radiative flux Q is

$$F = c\{[Q_{clrc} - Q_{clr}](1 - C) + [Q_{cldc} - Q_{cld}]C\}, \quad (1)$$

where the subscripts *clr* and *cld* refer to the mean clear and cloudy conditions, respectively, and *clrc* and *cldc* refer to those same quantities except that contrails are introduced into the atmospheric profile with a specified particle size and optical depth τ . To match available observations of persistent linear contrails [e.g., Mannstein *et al.* 1999], a normalized diurnal cycle of contrail coverage is applied to the mean contrail cover to estimate c at each hour. The diurnal cycle approximates the longitudinally dependent daily traffic distribution [Schmidt and Brunner 1997] with a global 2:1 day-night ratio which is typical for most regions except for 60°E where most traffic occurs during the night.

The shortwave (SW) and longwave (LW) radiative fluxes are computed at each hour for 24 hours using a 2.5°-latitude equal-area grid with 40 layers in the vertical. Longitudinal resolution is 2.5° at the Equator. Solar zenith angles and day length at the middle of the month are assumed to represent the entire month. Surface albedo and temperature are specified at the center of each local hour. Temperature and relative humidity are specified for each atmospheric layer. For the cloudy cases, cloud optical depth, phase, and particle size are specified at the mean altitude of the clouds at each hour. Radiative transfer calculations are performed assuming horizontally homogeneous conditions using the one-dimensional delta-2-stream radiative transfer code of Fu and Liou [1993] to compute the instantaneous SW and LW fluxes for the four conditions subscripted in (1). The results are

¹NASA Langley Research Center, Hampton, VA

²DLR Oberpfaffenhofen, Wessling, Germany

³Analytical Services and Materials, Inc., Hampton, VA

⁴NOAA, Aeronomy Laboratory, Boulder, CO

Copyright 1999 by the American Geophysical Union.

Paper number 1999GL900358.

0094-8276/99/1999GL900358\$05.00

averaged over the day for each region to estimate the monthly mean SW and LW fluxes. Contrail SW and LW forcing, F_{SW} and F_{LW} , respectively, are then computed with (1) and summed to obtain the net forcing F_{net} . The model resolves absorption and scattering by gases, aerosols, and particles in 6 SW and 12 LW bands. Meerkötter et al. [1999] compared the results of this model (in the 4-stream version) and two other established methods and found differences of up to 7% in radiative forcing, mainly because of different representations of ice particle properties in the three models.

The cloud amount, height, and optical depth are specified using the monthly mean 3-hourly D2 results of the International Satellite Cloud Climatology Project (ISCCP) [Rossow and Schiffer 1991], interpolated to 1 hour for 4 months (January, April, June, October) of 1986. The mean 1986 global ISCCP cloud cover is 68%. Ice clouds are modeled with randomly oriented hexagonal columns with effective diameters of 60 μm . Water clouds are modeled with droplets of 10- μm effective radius. Surface temperature and albedo are from the ISCCP data and Staylor and Wilber [1990], respectively. Liquid water clouds are specified for cloud temperatures greater than 253 K. Colder clouds are assumed to be composed of ice. Standard temperature and moisture profiles are assumed for pressures less than 50 hPa. Numerical weather analysis monthly mean profiles from the National Center for Environmental Prediction are used for pressures greater than 50 hPa. Continental and marine aerosols were included following the approach of Charlock and Alberta [1996] with a constant visible optical depth of 0.2 in all cases. The June 1986 calculations without contrails were compared to the corresponding monthly means measured by the Earth Radiation Budget Experiment [ERBE; see Barkstrom 1984] over the USA for 4 months. The mean model-based LW and SW fluxes are, respectively, $1 \pm 4 \text{ Wm}^{-2}$ and $3 \pm 6 \text{ Wm}^{-2}$ greater than the ERBE values. Most of the SW bias is due to the surface albedos. These results indicate that the contrail calculations use a realistic reference case.

The radiative properties of contrails depend on the shape and size spectrum of the ice crystals [Liou et al. 1998]. Most important, however, is the ice water path (IWP), i.e., the vertical integral of ice water content (IWC) over the geometrical depth of the contrails. In this study, contrails are assigned to a layer at 200 hPa and assumed to be 220-m thick with hexagonal ice columns having a 24- μm volume mean diameter. The IWP is adjusted such that the contrails have a parametrically prescribed solar optical depth τ of 0.1, 0.3, or 0.5 at 0.55- μm wavelength, which covers the range of observed values [Jäger et al. 1998; Meerkötter et al. 1999]. Since the actual IWC may depend on temperature, a case with IWC set to 50% of the water available for ice formation from vapor at 100% humidity relative to liquid saturation is also considered. This IWC prescription approximates the few IWC values that have been measured in contrails within a factor of about 3 [Meerkötter et al. 1999].

The global distribution of contrail cover is specified as computed for present meteorological conditions and for a traffic database of 1992 [Sausen et al. 1998] and an air traffic scenario of 2050 [Gierens et al. 1999b]. The temperature and humidity data used in the contrail estimates are taken from 11 years of the European Centre for Medium-Range Weather Forecast analysis data. The contrail cover is proportional to the product of the coverage by "possible contrail" air masses and the fuel consumption in those air masses. Possible contrail air masses are those that are cold and humid enough

such that aircraft flying within them induce persistent contrails. The fuel consumption rate serves as a measure of the number of aircraft causing contrails. The product is scaled to match the 0.5% mean contrail cover [Bakan et al. 1994] for the European/Atlantic region (30°W to 30°E, 35°N to 75°N). For 1992, the fuel consumption values are taken from Schmitt and Brunner [1997]. For 2050, the expected fuel consumption is taken from the reference scenario (Fa1) set up by a group of forecast experts [Forecasting and Economic Analysis Sub-Group (FESG) 1998]. Contrail formation depends on the overall propulsion efficiency (η) of the aircraft. The present calculations assume η equals 0.3 for 1992 and 0.5 for 2050 [Gierens et al. 1999a]. An increase of η from 0.3 to 0.5 reduces the specific fuel consumption per engine thrust by 40% and causes contrails to form, on average, at about 700-m lower flight altitude [Schumann 1996].

The computed annual mean contrail cover is 0.09% in the global mean with a local maximum of 5.5% over the eastern USA, a secondary maximum of 3.8% over northern Europe, and large values over the North Atlantic and in the Far East. In the scenario for 2050, total aviation fuel consumption increases 3.2-fold (4.4-fold above 500 hPa) compared to 1992. Contrails then cover 0.47% of the Earth if η is assumed to be 0.5 (0.38% for η of 0.3). Hence, contrail cover is expected to increase by a factor of about 5 (4.4 for η of 0.3) over present values, even for constant climate conditions. In 2050, the mean contrail coverage is maximal over Europe (4.6%, 4 times more than 1992), the USA (3.7%, 2.6 times more), and southeastern Asia (1.2%, 10 times more). The areal extent of contrails depends on wind shear, vertical motions, and existing cirrus cover, factors not included in this thermodynamic analysis.

Results

Global mean values of TOA radiative forcing calculations are summarized in Table 1. For all cases, F_{SW} is negative, while F_{LW} and F_{net} are positive. All three values increase a little less than linearly with τ . Figure 1 shows the global distribution of F_{net} for τ of 0.3 for 1992. The annual mean forcing is 0.02 Wm^{-2} with largest values in regions of strong air traffic. Maximum values occur in the dense air traffic zones over northeastern France (0.71 Wm^{-2}) and near New York (0.58 Wm^{-2}).

The absolute magnitude of F_{SW} increases with decreasing surface albedo. Therefore, F_{SW} is smaller for contrails forming above low-level clouds than over dark surfaces. For a given contrail coverage, F_{LW} is largest over warm surfaces and dry atmospheres. Therefore, F_{LW} decreases over cloudy areas as the cloud top altitude increases. For example, over low-level marine stratus clouds, F_{LW} will differ negligibly from the cloud-free ocean case because the sea surface is only a few degrees warmer than the cloud tops. The clouds are highly reflective, however, so F_{SW} will be much smaller than its value over the clear ocean. Thus, F_{net} over marine stratus regions should be strongly positive compared to other regions with the same contrail coverage. Conversely, F_{LW} and F_{net} will be minimal over cirrus clouds because the cirrus and contrails are at similar temperatures and the contrails only slightly increase the SW albedo. This cloud-height effect may explain why the contrail forcing over Europe is greatest despite the greater contrail coverage over the northeast USA. Cirrus cloudiness over Europe is approximately half that over the USA while the total cloudiness is approximately the same for both regions [Warren et al. 1986]. In the present model, F_{net} is positive

Table 1. Global mean top-of-atmosphere shortwave (SW), longwave (LW), and net radiative forcing (Wm^{-2}) by contrails in 1992 and in a 2050 scenario. Variable τ corresponds to ice water content (IWC) as a function of ambient temperature.

τ	1992			2050		
	SW	LW	Net	SW	LW	Net
0.1	-0.003	0.011	0.008	-0.018	0.067	0.049
0.3	-0.008	0.025	0.017	-0.049	0.148	0.099
0.5	-0.012	0.033	0.020	-0.075	0.197	0.122
variable	-0.004	0.014	0.010	-0.024	0.084	0.060

over the whole globe. The LW forcing probably outweighs F_{SW} , partly because it acts 24 hours each day and is often unaffected by cloud cover, while underlying cloudiness of any sort will substantially dampen the albedo impact of contrails.

The radiative imbalance induced by contrails is strongly dependent on latitude (Figure 2a). As expected from the concentration of air traffic at the northern mid-latitudes, 92% of the global contrail forcing is found in the Northern Hemisphere. The zonal mean forcing is largest near 40° to 50°N and exceeds the global mean by a factor of 5. The zonal mean specific forcing per unit contrail cover (Figure 2b) varies between 0.1 and 0.3 Wm^{-2} per % of contrail cover. It peaks over subtropical land because the surfaces are warm and have relatively high albedos. This quantity is also relatively large near 70°N where bright, snow-covered sea ice and low clouds are prevalent. There, the SW cooling by contrails is small, but the surface and low clouds are relatively warm compared to the upper troposphere and the atmosphere is dry enough such that a contrail will still cause significant LW forcing.

The relative global distribution of radiative forcing calculated for the 2050 scenario is similar to that shown in Figure 1. However, radiative forcing grows more strongly globally than in the current peak-traffic regions because of a greater increase in flights outside these areas. The global mean forcing is 0.1 Wm^{-2} for τ of 0.3 in 2050 with maximum values of 3.0 and 1.4 Wm^{-2} over northeastern France and the eastern USA (3.3 and 2.4 times more than 1992), respectively. The zonal dependence of the forcing and the contrail-cover specific forcing are similar for both 1992 and 2050 (see Figure 2). Overall, F_{SW} , F_{LW} , and F_{net} are about 6 times larger in 2050 than in 1992 (see Table 1). The radiative forcing increases

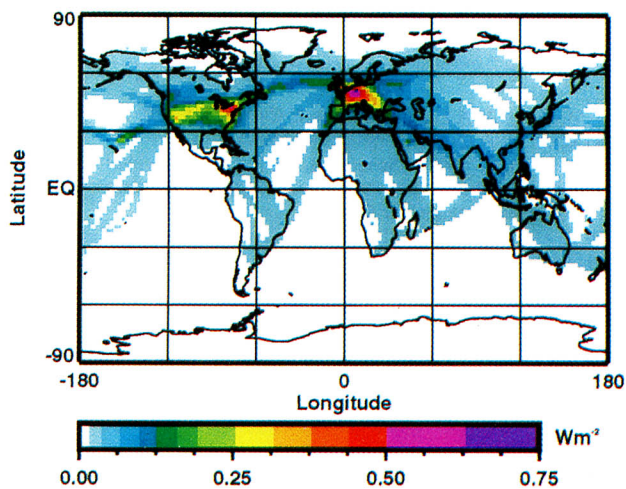


Figure 1. Annual mean net radiative forcing at the top of atmosphere for estimated 1992 contrail cover with $\tau = 0.3$.

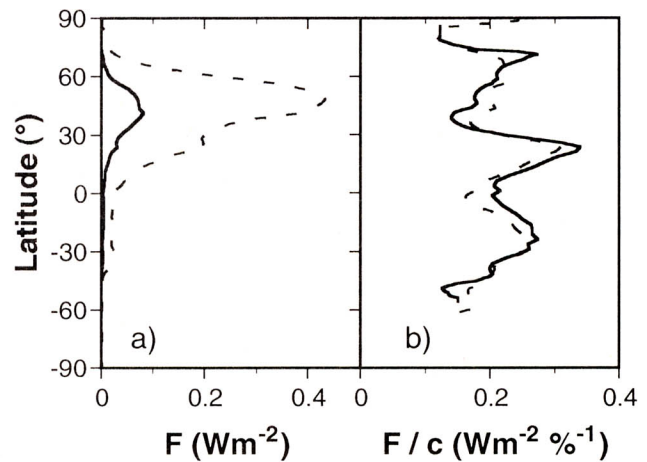


Figure 2. (a) Zonal-mean contrail net radiative forcing in Wm^{-2} for 1992 (solid) and 2050 (dashed). (b) Same per unit contrail cover (in %) for 1992 (solid) and 2050 (dashed).

more strongly than the contrail cover because of relatively large traffic increases over warm surfaces such as in the subtropics and over Asia.

Discussion

The computed results for global radiative forcing by contrails depend on the assumed values of the contrail cover and the mean optical depth of contrails. Neither is well known. For 1992, the computed global contrail cover was normalized to yield 0.5% observed cover by line-shaped contrails over Europe to match the satellite data. Satellite images mainly reveal the thicker linear contrails. Narrow or optically thin contrails and non-linear contrail cirrus are not accurately detected in such satellite data. Thus, the results for the larger τ values (0.3 to 0.5) are considered in combination with the given contrail cover (0.1% globally) as being most representative of the actual forcing conditions for the considered contrails. Hence, a 0.1% global increase in linear contrail cloud cover causes a radiative forcing of the Earth-atmosphere system of approximately 0.02 Wm^{-2} . The actual global cover may be 2 to 3 times smaller or larger than the derived line-shaped contrail cover [Gierens *et al.* 1999a] but is probably larger [e.g., Minnis *et al.* 1998]. The optical depth value is likely uncertain to a factor of 2 to 3 [Meerkötter *et al.* 1999]. Thus, assuming Gaussian behavior of the individual uncertainties, the radiative forcing value may differ from the given best estimate by a factor of about 4. This uncertainty estimate does not account for potential surprises that are conceivable because many parameter values, such as contrail overlap and particle size, are uncertain as a result of sparse observations. While the forcing also depends on cloud height distribution, the ERBE comparisons show that mean cloud height reasonably approximates contrail-free conditions.

The global radiative forcing by contrails is much smaller than that attributed to other anthropogenic changes in the last century ($\sim 1.5 \text{ Wm}^{-2}$ in 1992), but is comparable to the forcing by past aircraft emissions of carbon dioxide [Brasseur *et al.* 1998]. In steady state, the 1992 contrail coverage may increase the mean surface temperature by 0.01 to 0.02 K globally if the climate sensitivity due to contrail forcing is comparable to that of well-mixed greenhouse gases. Regionally, the radiative forcing is larger but the climate

response to this forcing may not be proportional to local forcing values and remains to be determined. Zonal-mean steady-state temperature changes between 0.01 and 0.1 K may be possible for present contrail cover when results of model studies are scaled to the contrail cover and radiative forcing found here [e.g., Liou et al. 1990, Ponater et al. 1996].

In the 2050 reference scenario of FESG [1998] with $\tau = 0.3$, the best estimate of global radiative forcing is 0.1 Wm^{-2} . The uncertainty range is larger than that for 1992 and is, at least, a factor of 4. The radiative forcing by contrails is computed to increase from 1992 to 2050 by a factor of 6 (0.099/0.0165 for $\tau = 0.3$, see Table 1). This factor results from the global increase in fuel consumption (factor 3.2), more traffic in the upper troposphere where contrails form preferentially (factor 1.24), more efficient engines (factor 1.24), and more contrails over areas with high specific radiative forcing (factor 1.11).

Concluding Remarks

The global distribution of radiative forcing by contrails has been estimated for 1992 and 2050, accounting for changes in contrail cover for future air traffic with fixed climatic conditions. Feedbacks of potential future climate changes on contrail and natural cloud cover are unknown. Also, older contrails that have developed and lost their linear shape add more contrail cover that has not yet been quantified. Finally, the indirect effects of aircraft emissions on the radiation budget such as due to changes in the properties of otherwise existing 'natural' cirrus clouds [Jensen and Toon 1997] may cause a radiative forcing comparable to that by line-shaped contrails [Wyser and Ström 1998]. Thus, the results presented here likely represent the minimum contrail effect. Further study is needed to estimate the maximum radiative forcing impact of contrails on climate.

Acknowledgments. This research is partially supported by the NASA Subsonic Assessment Program under the Atmospheric Effects of Aviation Project. The authors wish to thank Robert Sausen of DLR, for his comments and contributions to the simulated contrail dataset.

References

- Bakan, S., M. Betancor, V. Gayler, and H. Grassl, Contrail frequency over Europe from NOAA-satellite images, *Ann. Geophys.*, **12**, 962-968, 1994.
- Barkstrom, B. R., The Earth Radiation Budget Experiment (ERBE), *Bull. Amer. Meteorol. Soc.*, **65**, 1170-1185, 1984.
- Brasseur, G.P., R.A. Cox, D. Hauglustaine, I. Isaksen, J. Lelieveld, D.H. Lister, R. Sausen, U. Schumann, A. Wahner, and P. Wiesen, European scientific assessment of the atmospheric effects of aircraft emissions, *Atmos. Environ.*, **32**, 2327-2422, 1998.
- Charlock, T. P. and T. L. Alberta, The CERES/ARM/GEWEX Experiment (CAGEX) for the retrieval of radiative fluxes with satellite data, *Bull. Amer. Meteorol. Soc.*, **77**, 2673-2683, 1996.
- Forecasting and Economic Analysis Sub-Group (FESG), Report, obtainable from Air Transport Bureau, ICAO, 999 University Street, Montreal, Quebec, H3C 5H7, Canada, 1998.
- Fortuin, J.P.F., R. van Dorland, W.M.F. Wauben, and H. Kelder, Greenhouse effects of aircraft emissions as calculated by a radiative transfer model, *Ann. Geophys.*, **13**, 413-418, 1995.
- Fu, Q. and K.N. Liou, Parameterization of the radiative properties of cirrus clouds, *J. Atmos. Sci.*, **50**, 2008-2025, 1993.
- Gierens, K., R. Sausen, and U. Schumann, A diagnostic study of the global distribution of contrails. Part II: Future air traffic scenarios. *Theor. Appl. Climatol.*, in press, 1999a.
- Gierens, K., U. Schumann, M. Helten, H. Smit, and A. Marengo, A distribution law for relative humidity in the upper troposphere and lower stratosphere derived from three years of MOZAIC measurements, *Ann. Geophys.*, in press, 1999b.
- Jäger, H., V. Freudenthaler, and F. Homburg, Remote sensing of optical depth of aerosols and cloud cover related to air traffic, *Atmos. Environ.*, **32**, 3123-3127, 1998.
- Jensen, E. J., and O.B. Toon, The potential impact of soot particles from aircraft exhaust on cirrus clouds, *Geophys. Res. Lett.*, **24**, 249-253, 1997.
- Liou, K.-N., S.C. Ou, and G. Koenig, An investigation of the climatic effect of contrail cirrus, *Air Traffic and the Environment: Background, Tendencies, and Potential Global Atmospheric Effects* [U. Schumann (ed.)]. Springer-Verlag, Berlin, pp. 154-169, 1990.
- Liou, K.N., P. Yang, Y. Takano, K. Sassen, T. Charlock, and W. Arnott, On the radiative properties of contrail cirrus, *Geophys. Res. Lett.*, **25**, 1161-1164, 1998.
- Mannstein, H., R. Meyer, and P. Wendling, Operational detection of contrails from NOAA-AVHRR-data, *Int. J. Remote Sensing*, in press, 1999.
- Meerkötter, R., U. Schumann, D. R. Doelling, P. Minnis, T. Nakajima, and Y. Tsushima, Radiative forcing by contrails. *Ann. Geophys.*, in press, 1999.
- Minnis, P., J.K. Ayers, and S.P. Weaver, *Surface-Based Observations of Contrail Occurrence Frequency Over the U.S., April 1993 - April 1994*, NASA Reference Publ. 1404, 1997.
- Minnis, P., D.F. Young, D.P. Garber, L. Nguyen, W.L. Smith, Jr., and R. Palikonda, Transformation of contrails into cirrus during SUCCESS, *Geophys. Res. Lett.*, **25**, 1157-1160, 1998.
- Ponater, M., S. Brinkop, R. Sausen, and U. Schumann, Simulating the global atmospheric response to aircraft water vapour emissions and contrails: A first approach using a GCM, *Ann. Geophys.*, **14**, 941-960, 1996.
- Rossov, W. B. and R. A. Schiffer, ISCCP cloud data products. *Bull. Amer. Meteorol. Soc.*, **72**, 2-20, 1991.
- Sausen, R., K. Gierens, M. Ponater, and U. Schumann, A diagnostic study of the global distribution of contrails: Part I: Present day climate, *Theor. Appl. Climatol.*, **61**, 127-141, 1998.
- Schmitt, A. and B. Brunner, Emissions from aviation and their development over time, *DLR-Mitt. 97-04*, DLR, Köln, Germany, pp. 37-52, 1997.
- Schumann, U., 1996, On conditions for contrail formation from aircraft exhausts, *Meteor. Z.*, **5**, 4-23, 1996.
- Schumann, U. and P. Wendling, Determination of contrails from satellite data and observational results, *Air Traffic and the Environment* [U. Schumann (ed.)]. Springer-Verlag, Heidelberg, pp. 138-153, 1990.
- Staylor, W.F. and A.C. Wilber, Global surface albedo from ERBE data, *Proc. Seventh Conf. Atmospheric Radiation*, San Francisco, CA, July 23-27, Amer. Meteor. Soc., Boston, pp. 231-236, 1990.
- Warren, S. G., C. J. Hahn, J. London, R. M. Chervin, and R. L. Jenne, Global distribution of total cloud cover and cloud type amounts over land, NCAR Tech. Note *NCARTN-273+STR*, 229 pp., 1986.
- Wyser, K. and J. Ström, A possible change in cloud radiative forcing due to aircraft exhaust, *Geophys. Res. Lett.*, **25**, 1673-1676, 1998.

P. Minnis, NASA Langley Research Center, MS 420, Hampton, VA 23681-0001, USA (email: p.minnis@larc.nasa.gov).

K. M. Gierens and U. Schumann, DLR Oberpfaffenhofen, Institut für Physik der Atmosphäre, Postfach 1116, 82230 Wessling, Germany (email: ulrich.schumann@dlr.de).

D. R. Doelling, AS&M, Inc., NASA Langley Research Center, MS 936, Hampton, VA 23666 (email: d.r.doelling@larc.nasa.gov).

D. W. Fahey, NOAA, Aeronomy Laboratory, 325 Broadway, Boulder, CO 80303-3328, USA (fahey@al.noaa.gov).

(Received January 29, 1999; accepted March 24, 1999.)